

Luminaire Reference Points (LRP) in Visible Light Positioning using Hybrid Imaging-Photodiode (HIP) Receivers

Stefanie Cincotta
*Dept. of Electrical and
 Computer Systems Engineering
 Monash University
 Melbourne, Australia
 stefanie.cincotta@monash.edu*

Adrian Neild
*Dept. of Mechanical and
 Aerospace Engineering
 Monash University
 Melbourne, Australia
 adrian.neild@monash.edu*

Jean Armstrong
*Dept. of Electrical and
 Computer Systems Engineering
 Monash University
 Melbourne, Australia
 jean.armstrong@monash.edu*

Abstract—Visible Light Positioning (VLP) is an exciting new technology that has the potential to provide indoor positioning in a myriad of applications. Typically, VLP uses LED luminaires for positioning beacons and, like other positioning technologies, there is a requirement that sufficient beacons are available in the field of view (FOV) for triangulation. This can be challenging in many environments due to the luminaire placement and size. In this paper we investigate the use of luminaire reference points (LRPs) and hybrid imaging-photodiode (HIP) receivers to improve the reliability and robustness of VLP. LRP are precisely defined points on a luminaire that can be recognised by the imaging sensor in a HIP receiver. We show that, by associating multiple LRPs with a single luminaire, it is possible to achieve positioning when only one luminaire is in the FOV of the receiver. We demonstrate, using the geometric dilution of precision, that low positioning errors can be achieved even when luminaire geometry and spacing is non-ideal.

Index Terms—visible light positioning, angle of arrival, luminaire reference points, dilution of precision, hybrid imaging-photodiode receivers, QADA-plus

I. INTRODUCTION

The widespread introduction of LED indoor lighting has provided an opportunity to create a completely new form of indoor positioning: visible light positioning (VLP) [1]. This is possible because LEDs, unlike conventional lighting, can be modulated at megahertz frequencies and so can transmit data at very high rates. In Fig. 1, the smartphone contains a VLP receiver that is receiving data from the LED luminaires, enabling it to determine its location.

Ideally a VLP system should be ‘stand-alone’ like GPS. A stand-alone VLP system would allow anyone with the appropriate receiver to determine their position using only information from the nearby luminaires. This means that the system should not require any other sensors, or any prior fingerprinting, or access to any external databases.

This work was supported by the Australian Research Council’s (ARC) Discovery funding schemes (DP150100003 and DP180100872) and an Australian Government Research Training Program (RTP) Scholarship.

978-1-7281-1788-1/19/\$31.00 © 2019 Crown

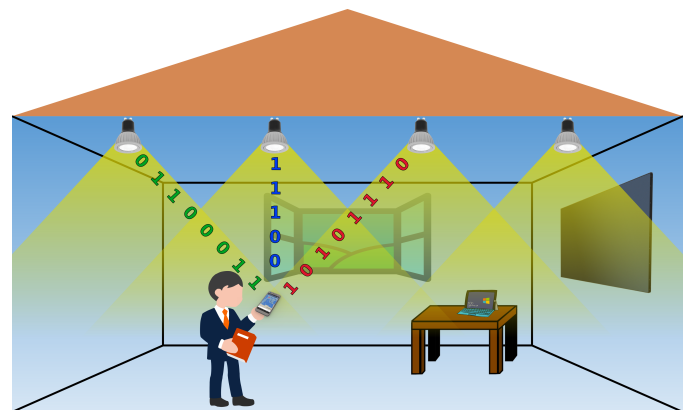


Fig. 1. Indoor VLP scenario

Despite the apparent potential of VLP and extensive worldwide research [2]–[4], experimental verification of the accuracy of stand-alone VLP systems is only just being addressed [5], [6]¹. This is because a VLP receiver must perform two distinct functions: it must receive data from each of the transmitting luminaires², which contains information about the position of that luminaire, and it must be able to determine either its distance from, or the direction to each luminaire.

To date most of the VLP receivers which have been described for stand-alone systems can be divided into two general categories: photo-diode based receivers (PDRs) [7]–[9] and imaging receivers (IMRs) [10]–[12]. Because the bandwidth of photodiodes is very wide, PDRs can be designed to receive very high data rates. For example, visible light communication systems (VLC) are available with multi-megabit per second

¹Although there are many papers that claim accurate positioning using PDRs, many make unrealistic assumptions, see [5] for a detailed discussion of the practical limitations.

²Luminaire is the technical term for a light fitting. A luminaire is typically made up of many LEDs. We use this term instead of ‘light’ to avoid confusion with the multiple meanings of ‘light’.

data rates [13]. This is far in excess of the rates needed in VLP. However, the limitation of PDRs is their inability to accurately estimate either the distance, or the direction, of the transmitting luminaires.

In contrast IMRs, which typically use a camera as the receiver, can accurately determine the direction to any feature which can be identified in the image. If a luminaire can be identified in the image, its direction can be estimated. However it is difficult to receive high speed data using a camera, and despite clever work-arounds, such as using the rolling-shutter mechanisms of many digital cameras [10], [14], data rates are, at best, a few kilobits per second, which limits the ability of each luminaire to transmit detailed information about its position.

Very recently a new class of receiver has been described: the hybrid imaging-photodiode (HIP) receiver [5]. The HIP receiver has an imaging sensor which enables the precise direction to each luminaire to be estimated and a photodiode section which receives the high speed data and provides enough directional accuracy to determine which luminaire in the image has transmitted that data. By combining the information from the two receiver sections, the HIP receiver can both receive high speed data and obtain position information relative to the source of that data. In [5] we described, in detail, one particular form of HIP: the QADA-plus. The HIP receiver, more generally, is described in more detail in Section II.

For position estimates to be made, either triangulation or trilateration is required. Until now this has meant that at least three luminaires must be within the field of view (FOV) of the VLP receiver: a requirement that will frequently not be met in indoor environments. In this paper we show that the introduction of luminaire reference points (LRP) removes this limitation and makes it possible to create a stand-alone VLP system which requires only a single luminaire within its FOV. LRPs are simply markers, illuminated or otherwise, on the luminaires, the locations of which can be transmitted as part of the high speed data stream.

This paper analyzes a positioning system using a HIP receiver and LRPs. The accuracy of the position estimation, based on angle of arrival (AOA) measurement used in the HIP receiver, depends on both the accuracy of the AOA estimates for each of the LRPs and the effect of geometric dilution of precision (GDOP). Because LRPs located on a single luminaire will inevitably be close together and so will only have small angular differences, GDOP will inevitably cause more degradation than for the case when different transmitting luminaires are used as beacons. However, the errors in AOA estimates for the LRPs based on high resolution images can be very small.

This paper shows that the new system, using a HIP receiver and LRPs, can provide very accurate stand-alone position estimation, even in the most challenging of environments. We provide a solution to the problem caused by realistic luminaire installations, where it can be difficult to capture enough beacons in the FOV to be able to triangulate. Additionally, we present results demonstrating that low uniform error across a

large region is possible when four LRPs are associated with each luminaire.

II. REFERENCE POINTS

A. Luminaire reference points and HIP receivers

The power of the combination of LRPs and HIPs depends on the detailed properties of each. HIPs are required for LRPs to be used. LRPs increase the accuracy and reliability of HIP position estimates.

The three different properties of the HIP receiver which combine to make the use of LRPs possible are:

- 1) The HIP can receive the high speed data which is transmitted by each luminaire in the form of beacon information packets (BIPs) [5], [15]. BIPs are discussed in more detail below. The BIPs transmitted by each luminaire give information about the type and position of each of the LRPs in that luminaire.
- 2) The PD section of the HIP can produce accurate enough AOA information for each luminaire to be uniquely identified in the image.
- 3) The high resolution images output from the imaging section of the HIP allow each LRP to be identified, even if each is quite small.

The use of LRPs greatly improves the accuracy and reliability of HIP based positioning because:

- 1) LRPs are precisely defined positions on the image, whereas the position of the centroid of a luminaire may be difficult to estimate [5].
- 2) Each luminaire may contain several LRPs so that triangulation can be achieved even if only one luminaire is within the receiver FOV.

B. Luminaire reference points

LRPs are features associated with a luminaire which can be detected in an image. They were first described in [15] and a more detailed discussion was included in [5], but this is the first work to consider in detail their potential to dramatically improve the performance of VLP systems.

LRPs can take many forms, and the design of LRPs for future VLP systems is likely to be an important new research area. Examples of possible LRPs include a single different coloured LED within a luminaire (see Fig. 2), or a small mark on a luminaire frame. Our discussions with luminaire manufacturers and lighting designers have suggested that either option would be acceptable. In fact, it has been suggested that a different coloured LED could be a sales feature as it would indicate that the luminaire was a state-of-the art VLP enabled luminaire.

The crucial aspect of an LRP is that the receiver must be able to detect it in an image, but this detection task is made much simpler due to the properties of the HIP receiver. The HIP receiver knows what types of LRPs are associated with each luminaire, as this is contained in the information transmitted by the luminaire, and a HIP receiver also knows the approximate position of each luminaire as this too can

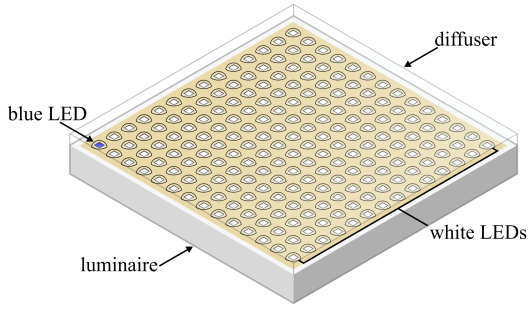


Fig. 2. A square luminaire consisting of a large array of white LEDs with a single blue LED in the corner.

be provided by the photodiode based detection. This means that the image processing program, used to detect the exact position of an LRP, knows what to look for and approximately what region of the image to search.

The size and shape of reference points can be designed to optimize their identification by the camera section of the HIP. For example, it may be advantageous to choose shapes for which there are highly optimized image processing algorithms, such as circles.

C. HIP Receivers

Fig. 3 is a block diagram showing how HIP receivers are used in conjunction with LRPs. The LED luminaires transmit the BIPs which are packets of data containing information about the positions of their LRPs in a world coordinate system as well as the additional information needed to identify the LRPs. The PDR demodulates and decodes this data and also estimates the AOA. The AOA estimation makes it possible to match the decoded data with the relevant luminaire in the image. The decoded BIP and corresponding AOA estimate is passed to the image processing program. After processing, the image coordinates of the LRPs will have been matched to their respective world coordinates. Assuming sufficient LRPs have been identified in the image then the position of the receiver can be calculated using a triangulation algorithm.

The limitation in accuracy of positioning comes from the accuracy of detection of the LRPs in the image, and much

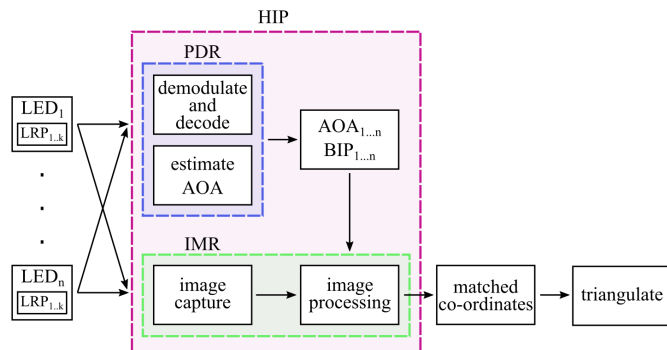


Fig. 3. Block diagram of a HIP receiver

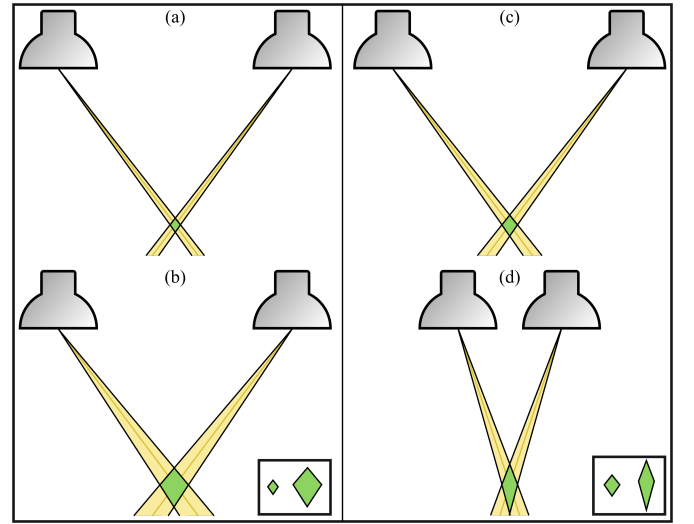


Fig. 4. Position error, shown as the green diamond, increases when the uncertainty in angle estimation increases (a and b) or when the angular separation between the beacons decreases (c and d)

more significantly, the triangulation that then follows.

QADA-plus [15] is a HIP receiver that combines a quadrature angular diversity aperture (QADA) receiver with a camera. The QADA uses a quadrant PD located below an aperture to form an angular diversity receiver [16]. Whilst QADA-plus was the first HIP receiver to be described, the general concept of HIP receivers applies more broadly to any PDR/IMR combination.

III. DILUTION OF PRECISION

The position dilution of precision has been used extensively in the analysis of optimal satellite position in GNSS [17]–[19]. In this section, we use the GDOP because, unlike satellite positioning, AOA positioning does not have a dependence on time. The GDOP relates the position error to the measurement error [20]. In Fig. 4 a simple 2-D representation is shown where the overlap area of the two rays of lights represent the position error. In Fig. 4 (a), the uncertainty in the AOA estimation is small, and thus the overlap is small. However, in (b), when the uncertainty is large, the overlap becomes much larger. For clarity, the two overlap areas are shown side by side below (b).

If the uncertainty in AOA is kept fixed, but the beacons are moved closer together and the angular separation decreases, the overlap area will also increase. This is shown in Fig. 4 (c) and (d), where it is most obvious when comparing the two diamonds in the bottom right corner. This demonstrates the problem when beacon placement is not ideal, but rather real and constrained by the geometry of the luminaire.

The GDOP is a function of the position in the three-dimensional space and it is defined as:

$$GDOP(x, y, z) = \sqrt{\text{tr}[(H^T H)^{-1}]} = \frac{\sigma_p(x, y, z)}{\sigma_a}. \quad (1)$$

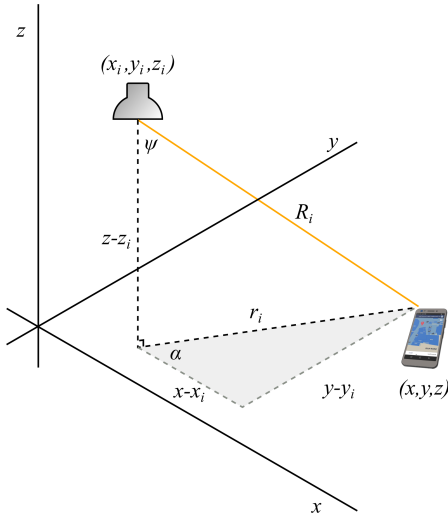


Fig. 5. The relationship between the angle of arrival and the position

where H is the geometric design matrix, $\text{tr}[\cdot]$ is the trace operator, σ_p is the standard deviation of the position error and σ_a is the standard deviation of the angle estimation error.

To construct the geometric design matrix, we first need to relate the AOA to the position in x , y , and z . From Fig. 5, it can be seen that if the receiver is located at position (x, y, z) and the i^{th} transmitter is located at (x_i, y_i, z_i) . Thus, the incident angle and polar angles are given by

$$\psi = \arctan\left(\frac{r_i}{|z - z_i|}\right) \quad (2)$$

and

$$\alpha = \arctan\left(\frac{y - y_i}{x - x_i}\right), \quad (3)$$

where $r_i = \sqrt{(x - x_i)^2 + (y - y_i)^2}$ is the two-dimensional Euclidean distance on the xy plane between the transmitter and receiver

As described in [21], the geometric design matrix is formulated using the partial derivatives of the incident and polar angle with respect to x , y and z . The geometric design matrix is first defined for each angle, and then combined into an augmented matrix. For the incident angle, from (2), we can determine that H_ψ is

$$\begin{bmatrix} \partial\psi_1 \\ \vdots \\ \partial\psi_n \end{bmatrix} = [H_\psi] \begin{bmatrix} \partial x \\ \partial y \\ \partial z \end{bmatrix} = \begin{bmatrix} \frac{\partial\psi_1}{\partial x} & \frac{\partial\psi_1}{\partial y} & \frac{\partial\psi_1}{\partial z} \\ \vdots & \vdots & \vdots \\ \frac{\partial\psi_n}{\partial x} & \frac{\partial\psi_n}{\partial y} & \frac{\partial\psi_n}{\partial z} \end{bmatrix} \begin{bmatrix} \partial x \\ \partial y \\ \partial z \end{bmatrix}. \quad (4)$$

Similarly, for the polar angle, using (3), we get

$$\begin{bmatrix} \partial\alpha_1 \\ \vdots \\ \partial\alpha_n \end{bmatrix} = [H_\alpha] \begin{bmatrix} \partial x \\ \partial y \\ \partial z \end{bmatrix} = \begin{bmatrix} \frac{\partial\alpha_1}{\partial x} & \frac{\partial\alpha_1}{\partial y} & \frac{\partial\alpha_1}{\partial z} \\ \vdots & \vdots & \vdots \\ \frac{\partial\alpha_n}{\partial x} & \frac{\partial\alpha_n}{\partial y} & \frac{\partial\alpha_n}{\partial z} \end{bmatrix} \begin{bmatrix} \partial x \\ \partial y \\ \partial z \end{bmatrix}. \quad (5)$$

Therefore, for a position with n LRP in the FOV, from (4) and (5), the geometric design matrix is given by:

$$[H] = \begin{bmatrix} \frac{(y_1 - y)}{r_1^2} & \frac{(x - x_1)}{r_1^2} & 0 \\ \vdots & \vdots & \vdots \\ \frac{(y_n - y)}{r_n^2} & \frac{(x - x_n)}{r_n^2} & 0 \\ \frac{|z_1 - z|(x_1 - x)}{r_1 R_1^2} & \frac{|z_1 - z|(y_1 - y)}{r_1 R_1^2} & \frac{r_1}{R_1^2} \\ \vdots & \vdots & \vdots \\ \frac{|z_n - z|(x_n - x)}{r_n R_n^2} & \frac{|z_n - z|(y_n - y)}{r_n R_n^2} & \frac{r_n}{R_n^2} \end{bmatrix}, \quad (6)$$

where $R_i = \sqrt{(x - x_i)^2 + (y - y_i)^2 + (z - z_i)^2}$ is the three-dimensional Euclidean distance between the transmitter and receiver.

IV. POSITIONING ERROR IN CHALLENGING ENVIRONMENTS

The following simulation results show the positioning error distribution for varying beacon geometries. Initially, we use a worst-case value of $\sigma_a = 1^\circ \approx 0.017$ rad. If a different value was used, the figures would be directly scaled due to the definition of the GDOP in (1). To illustrate this, we repeat the corridor simulations with $\sigma_a = 0.5^\circ \approx 0.0087$ rad. The value for σ_a has been reported over a wide range of values in the literature [21], [22]. In practice, the angular precision of a camera will be related to the lens quality, the number of pixels and the camera calibration.

A. Corridor Simulation

Corridors are particularly challenging environments for VLP. Building standards often allow them to have lower illumination requirements than other rooms [23] and combining that with their long, narrow geometry, the luminaires tend to be installed sparsely. Fig. 6 shows three different corridors, with three different LED luminaire installations, all located within a single building. The first two have rectangular batten luminaires that are installed with opposite orientations. The third one has square luminaires. The images are taken with a camera orientated in a vertical plane, and so very different to a receiver handset, such as a smart phone, which likely is held close to a horizontal plane. The FOV of the receiver would need to be very large to consistently have three luminaires in the FOV of the receiver, thus the following simulation results consider the case where four LRP are associated with each luminaire, one LRP in each corner. With the inclusion of these LRP the requirement is reduced so that only one luminaire need be in the FOV.

The corridor segment used in the simulation is an 8 metre section with a width of 1.8 metres. The corridor contains two luminaires, spaced 4.5 metres apart. In the first two cases, the luminaires have dimensions 120 cm \times 60 cm and in the third case the luminaires have dimensions 85 cm \times 85 cm. These rectangular dimensions correspond to the commercially available Philips Coreview Troffer luminaires. The dimensions of the square luminaire are chosen so that the area is the same



Fig. 6. Three different corridors with three different luminaire shapes

as the rectangular luminaires. Thus, the average illumination levels in the corridors would be equal in all cases. Whilst similar to the types of corridors shown in Fig. 6, the simulation parameters do not match exactly.

The FOV of the camera is 97° , which is the same FOV as the wide-angle front camera in a Google Pixel 3. For simplicity, we assume that the camera sensor is square and that the sensor's axes are aligned with the corridor's axes. The receiver is assumed to be held parallel to the ceiling and 0.7 m above the floor, which means that 5.2×5.2 m of the ceiling is visible. At all positions in the corridor there will be at least three LRPs in the FOV of the receiver which is sufficient to allow triangulation.

 TABLE I
 CORRIDOR SIMULATION PARAMETERS

Parameter	Value
Corridor dimensions	$800 \times 180 \times 300$ cm
Receiver Height	70 cm
Luminaire centroids	(170, 90, 300) & (630, 90, 300) cm
Rectangle Luminaire dimensions	86×86 cm
Square Luminaire dimensions	120×60 cm
FOV	97°
Angular precision (σ_a)	$1^\circ, 0.5^\circ$

For ease of comparison, all three figures in both Fig. 7 and Fig. 8 use the same scale. The black dots represent the positions of the LRPs and the dotted lines represent the outline of the luminaires. The simulation parameters are summarized in Table I.

In Fig. 7 (a), the distribution of the positioning error is shown for the case where the rectangular luminaires are parallel to the length of the corridor. In the central 2 m of the corridor, the error is much lower. In these positions, the receiver FOV encompasses LRPs from both luminaires. This provides a better geometry for the positioning beacons. In the

other regions of the corridor, the receiver is only able to use the LRPs from a single luminaire – note in these areas, in the absence of LRPs, positioning could not be achieved.

Fig. 7 (b) shows the distribution of positioning error when the rectangular luminaires are installed perpendicular to the corridor length. The area in between the luminaires where the receiver is able to capture LRPs from both luminaires is much smaller now due to the orientation of the luminaires, however overall the error distribution is more uniform. This is reflected in the standard deviation, as seen in Table II, which is much lower for this geometry compared to others.

Fig. 7 (c) shows a distribution that is similar to Fig. 7 (a). The central region of relatively low error is large, but there are also regions of relatively high error. Overall, this beacon arrangement performs the worst, with the largest mean and standard deviations.

In Fig. 8 the angular precision is now 0.5° . As can be seen, all the figures have been scaled by half, making the positioning error distribution much better. This demonstrates how the system can be improved with more accurate AOA estimates which could be the result of improvements in camera quality, image processing or LRP design.

 TABLE II
 CORRIDOR POSITIONING ERROR

σ_a	Min (cm)	Max (cm)	Mean (cm)	St. dev. (cm)
Rectangle - parallel				
$\sigma_a = 1^\circ$	4.46	11.36	6.55	1.25
$\sigma_a = 0.5^\circ$	2.23	5.68	3.28	0.63
Rectangle - perpendicular				
$\sigma_a = 1^\circ$	4.15	9.76	6.56	0.98
$\sigma_a = 0.5^\circ$	2.08	4.88	3.28	0.49
Square				
$\sigma_a = 1^\circ$	4.66	11.35	6.89	1.29
$\sigma_a = 0.5^\circ$	2.33	5.67	3.44	0.64

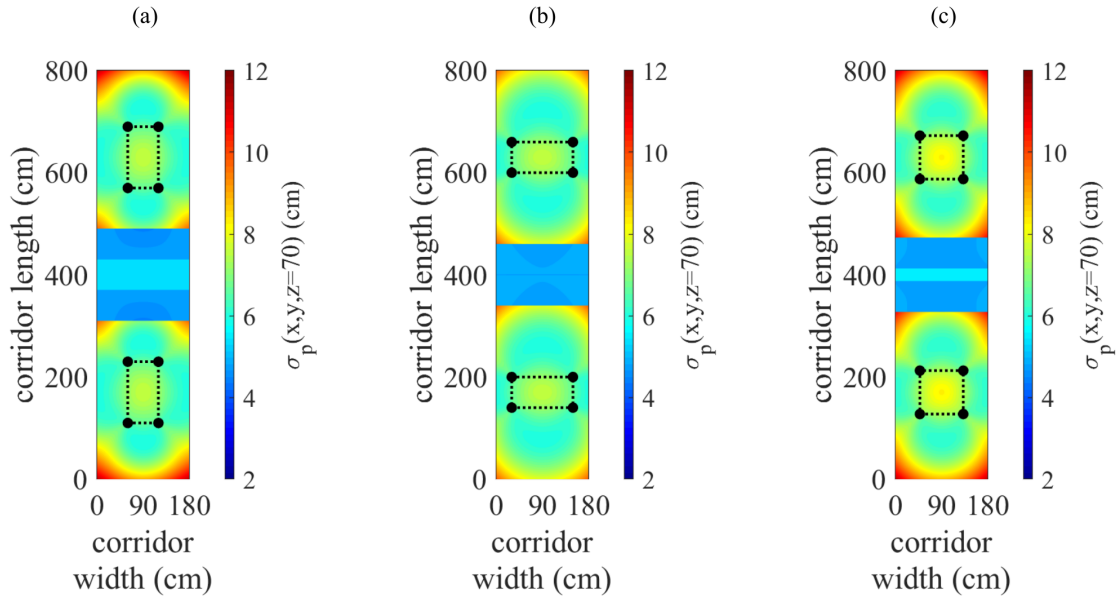


Fig. 7. Positioning error distribution ($\sigma_a = 1^\circ$) in a corridor for three different luminaire geometries: (a) rectangular luminaires with parallel alignment, (b) rectangular luminaires with perpendicular alignment and (c) square luminaires

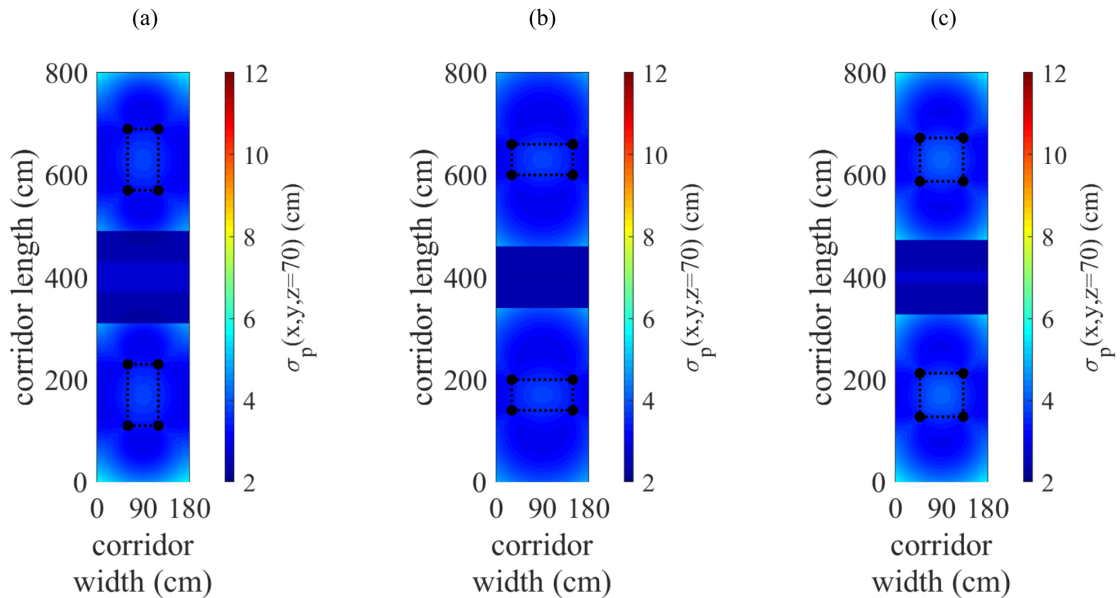


Fig. 8. Positioning error distribution ($\sigma_a = 0.5^\circ$) in a corridor for three different luminaire geometries: (a) rectangular luminaires with parallel alignment, (b) rectangular luminaires with perpendicular alignment and (c) square luminaires

B. Large open space simulation

Large rooms, such as warehouses, supermarkets or museums, are common places that could benefit from indoor positioning. Like many commercial or public buildings, these spaces typically have large luminaires. In the following simulations we consider an area with dimensions of $6 \text{ m} \times 6 \text{ m} \times 3 \text{ m}$. This area contains four square luminaires with dimensions $60 \text{ cm} \times 60 \text{ cm}$. The luminaires centroids are located at $(150,150,300)$, $(150,450,300)$, $(150,450,300)$ and $(450,450,300)$ cm. The receiver FOV is the same as in the

previous section and, again for ease of comparison, the figures all share the same scale.

In the first case, there is a single LRP in the centre of each luminaire. This would be similar to systems not using LRPs which typically rely on identifying the centroids of the luminaires. As can be seen in Fig. 9 the positioning error distribution was low and uniform. However, the region over which positioning is possible is very small. Only the central section, measuring approximately $2.2 \text{ m} \times 2.2 \text{ m}$, has sufficient beacons in the FOV. This is obviously not a viable

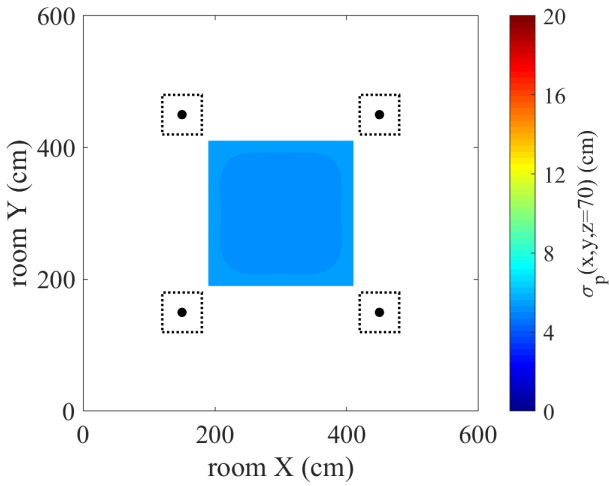


Fig. 9. Positioning error distribution for square luminaires with one LRP in a 6 m square area.

beacon geometry for a space of this size. Either the receiver FOV would need to increase substantially, or more beacons would need to be available. As it is not always possible to change the infrastructure to increase the luminaire density, then the addition of additional LRPs to the luminaires can provide a highly efficient solution to the problem.

In Fig. 10, the same area and luminaires are used, however there are now two LRPs on each luminaire, located in opposite corners. The positioning errors are very low in many parts of the room and fairly uniform. As seen in the previous scenario with corridors, the lowest errors occur when LRPs from different luminaires are in the FOV. The important feature here is that, through this small addition, it is now possible to position over a much larger region. This is a significant improvement, however it can be improved further by adding

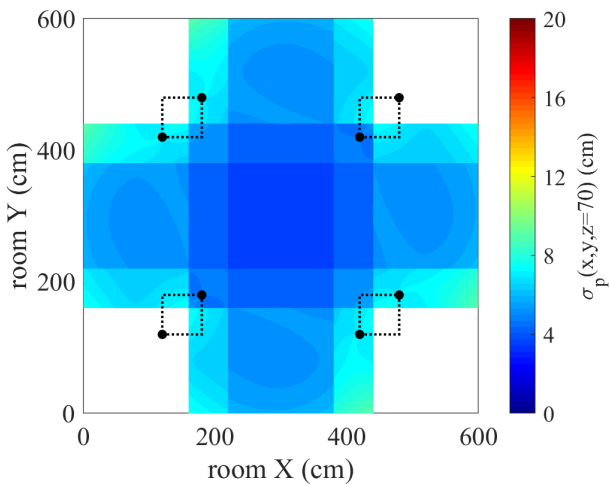


Fig. 10. Positioning error distribution for square luminaires with two LRPs in a 6 m square area

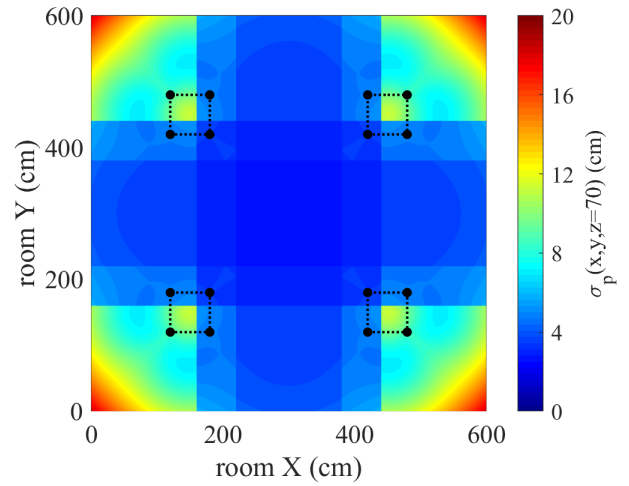


Fig. 11. Positioning error distribution for square luminaires with four LRPs in a 6 m square area

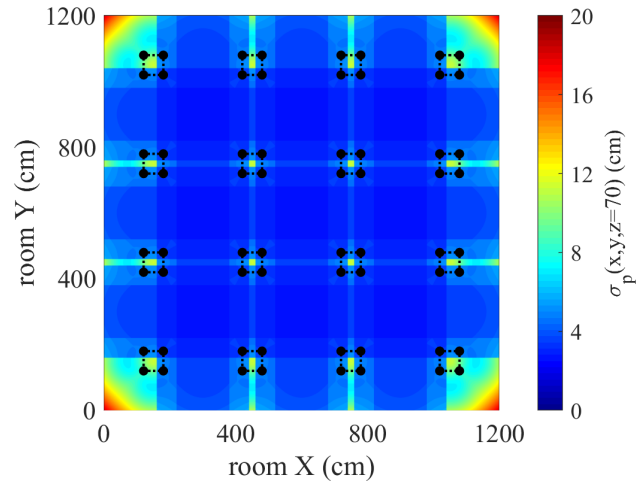


Fig. 12. Positioning error distribution over a larger region

LRPs to the remaining two corners of each luminaire.

Fig. 11 shows the result when four LRPs are on each luminaire. It is now possible to position in all regions of the area, though the errors are larger in the outer corners. The mean positioning error is similar to the previous two scenarios, however the standard deviation has increased due to those outer regions. Although the errors in the outer corners are relatively large, it is important to remember that it was not possible to localise in that region at all previously.

In Fig. 12, this area is tessellated to form a larger room with a continuation of the luminaire layout pattern. It can be seen that the resultant distribution of errors is low and uniform for much of the room, with larger errors occurring directly under the luminaires and in the corners. The reason that the area under the luminaires has larger errors is because it suffers from small angular separation between the LRPs. A summary of the results can be seen in Table III.

TABLE III
LARGE AREA POSITIONING ERROR

LRPs	Min (cm)	Max (cm)	Mean (cm)	St. dev. (cm)
area = 6 m × 6 m				
1	5.21	5.54	5.29	0.07
2	3.68	9.10	5.51	1.19
4	2.60	18.17	5.54	3.03
area = 12 m × 12 m				
4	2.60	18.16	4.08	2.00

V. CONCLUSION

In this paper, we have shown the advantage of using LRPs in VLP. In particular, we have shown how a HIP receiver can be used in conjunction with LRPs to overcome a major challenge in VLP – the requirement that at least three luminaires are visible in the FOV of the receiver. We have shown that that requirement can be reduced down to one single luminaire that contains at least three LRPs. This removes the need to increase the FOV of the receiver which can be challenging in compact receivers [24], [25].

One important advantage of VLP is the low demand on additional infrastructure. Instead of deploying a large number of single purpose beacons, such as in radio-frequency indoor positioning [26], a simple change of luminaire to ‘VLP-enabled’ luminaires is all that is needed. However, as existing buildings upgrade to LED illumination, the preference to retrofit will mean that the location and shape of the luminaires will often be far from ideal for positioning. In these cases, the use of LRPs instead of luminaire centroids dramatically increases the likelihood that positioning will be possible. An example of a common challenging luminaire installation was highlighted in this paper: corridors. Even in this degenerate case, we showed that, by using LRPs, acceptable positioning accuracy can be achieved.

To take advantage of LRPs, the receiver should ideally be a HIP. A HIP receiver takes advantage of the strengths of both PDRs and IMRs. QADA-plus is one form of HIP that has the significant advantage of being very compact. It could be easily integrated into a smartphone or exist in a small stand-alone receiver unit.

Using LRPs with HIP receivers means VLP has the potential to be implemented in most indoor locations.

REFERENCES

- [1] J. Armstrong, Y. A. Sekercioglu, and A. Neild, “Visible light positioning: a roadmap for international standardization,” *IEEE Communications Magazine*, vol. 51, no. 12, pp. 68–73, Dec. 2013.
- [2] B. Jang and H. Kim, “Indoor Positioning Technologies Without Offline Fingerprinting Map: A Survey,” *IEEE Communications Surveys Tutorials*, pp. 1–1, 2018.
- [3] J. Luo, L. Fan, and H. Li, “Indoor Positioning Systems Based on Visible Light Communication: State of the Art,” *IEEE Communications Surveys Tutorials*, vol. 19, no. 4, pp. 2871–2893, Fourthquarter 2017.
- [4] Y. Zhuang et al., “A Survey of Positioning Systems Using Visible LED Lights,” *IEEE Communications Surveys Tutorials*, vol. 20, no. 3, pp. 1963–1988, thirdquarter 2018.
- [5] S. Cincotta, C. He, A. Neild, and J. Armstrong, “Indoor Visible Light Positioning: Overcoming the Practical Limitations of the Quadrant Angular Diversity Aperture Receiver (QADA) by Using the Two-Stage QADA-Plus Receiver,” *Sensors*, vol. 19, no. 4, p. 956, Jan. 2019.
- [6] J. Armstrong, A. Neild, and S. Cincotta, “Visible light positioning receiver arrangement and two stage positioning method,” 2018902351, 2018.
- [7] B. Zhu, J. Cheng, Y. Wang, J. Yan, and J. Wang, “Three-Dimensional VLC Positioning Based on Angle Difference of Arrival With Arbitrary Tilting Angle of Receiver,” *IEEE Journal on Selected Areas in Communications*, vol. 36, no. 1, pp. 8–22, Jan. 2018.
- [8] S. Cincotta, C. He, A. Neild, and J. Armstrong, “High angular resolution visible light positioning using a quadrant photodiode angular diversity aperture receiver (QADA),” *Opt. Express*, OE, vol. 26, no. 7, pp. 9230–9242, Apr. 2018.
- [9] H. Steendam, “A 3D Positioning Algorithm for AOA-Based VLP with an Aperture-Based Receiver,” *IEEE Journal on Selected Areas in Communications*, vol. 36, no. 1, pp. 23–33, Jan. 2018.
- [10] Y.-S. Kuo, P. Pannuto, K.-J. Hsiao, and P. Dutta, “Luxapose: indoor positioning with mobile phones and visible light,” in *Proceedings of the Annual International Conference on Mobile Computing and Networking, MOBICOM*, Maui; United States, 2014, pp. 447–458.
- [11] M. H. Bergen, X. Jin, D. Guerrero, H. A. L. F. Chaves, N. V. Fredeen, and J. F. Holzman, “Design and Implementation of an Optical Receiver for Angle-of-Arrival-Based Positioning,” *Journal of Lightwave Technology*, vol. 35, no. 18, pp. 3877–3885, Sep. 2017.
- [12] R. Zhang, W. D. Zhong, K. Qian, and D. Wu, “Image Sensor Based Visible Light Positioning System With Improved Positioning Algorithm,” *IEEE Access*, vol. 5, pp. 6087–6094, 2017.
- [13] H. Haas, L. Yin, Y. Wang, and C. Chen, “What is LiFi?,” *Journal of Lightwave Technology*, vol. 34, no. 6, pp. 1533–1544, Mar. 2016.
- [14] H.-Y. Lee, H.-M. Lin, Y.-L. Wei, H.-I. Wu, H.-M. Tsai, and K. C.-J. Lin, “RollingLight: Enabling Line-of-Sight Light-to-Camera Communications,” in *Proceedings of the 13th Annual International Conference on Mobile Systems, Applications, and Services*, New York, NY, USA, 2015, pp. 167–180.
- [15] S. Cincotta, C. He, A. Neild, and J. Armstrong, “QADA-PLUS: A Novel Two-Stage Receiver for Visible Light Positioning,” in *2018 International Conference on Indoor Positioning and Indoor Navigation (IPIN)*, 2018, pp. 1–5.
- [16] S. Cincotta, A. Neild, C. He, and J. Armstrong, “Visible Light Positioning Using an Aperture and a Quadrant Photodiode,” in *2017 IEEE Globecom Workshops (GC Wkshps)*, 2017, pp. 1–6.
- [17] B. Huang, Z. Yao, X. Cui, and M. Lu, “Dilution of Precision Analysis for GNSS Collaborative Positioning,” *IEEE Transactions on Vehicular Technology*, vol. 65, no. 5, pp. 3401–3415, May 2016.
- [18] Y. Lu, D. Zhongliang, Z. Di, and H. Enwen, “Quality assessment method of GNSS signals base on multivariate dilution of precision,” in *2016 European Navigation Conference (ENC)*, 2016, pp. 1–6.
- [19] W. Huihui, Z. Xingqun, and Z. Yanhua, “Geometric dilution of precision for GPS single-point positioning based on four satellites,” *Journal of Systems Engineering and Electronics*, vol. 19, no. 5, pp. 1058–1063, Oct. 2008.
- [20] A. G. Dempster, “Dilution of precision in angle-of-arrival positioning systems,” *Electronics Letters*, vol. 42, no. 5, pp. 291–292, Mar. 2006.
- [21] M. H. Bergen, A. Arafa, X. Jin, R. Klukas, and J. F. Holzman, “Characteristics of Angular Precision and Dilution of Precision for Optical Wireless Positioning,” *Journal of Lightwave Technology*, vol. 33, no. 20, pp. 4253–4260, Oct. 2015.
- [22] T. Sun, F. Xing, and Z. You, “Optical System Error Analysis and Calibration Method of High-Accuracy Star Trackers,” *Sensors (Basel)*, vol. 13, no. 4, pp. 4598–4623, Apr. 2013.
- [23] “AS/NZS 1680.2.4:2017 Interior and workplace lighting Industrial tasks and processes.”
- [24] T. Kim, L. Yong, and Q. Xu, “Robust design study on the wide angle lens with free distortion for mobile lens,” in *AOPC 2017: Optical Storage and Display Technology*, 2017, vol. 10459, p. 104590Y.
- [25] B. Ma, K. Sharma, K. P. Thompson, and J. P. Rolland, “Mobile device camera design with Q-type polynomials to achieve higher production yield,” *Optics Express*, vol. 21, no. 15, p. 17454, Jul. 2013.
- [26] Y. Zhuang, J. Yang, Y. Li, L. Qi, and N. El-Sheimy, “Smartphone-Based Indoor Localization with Bluetooth Low Energy Beacons,” *Sensors*, vol. 16, no. 5, p. 596, Apr. 2016.